

From Magnitudes to Diameters: The Albedo Distribution of Near Earth Objects and the Earth Collision Hazard

A. Morbidelli

Observatoire de la Côte d'Azur, Boulevard de l'observatoire, B.P. 4229, 06304 Nice Cedex 4, France
E-mail: morby@obs-nice.fr

R. Jedicke

Lunar and Planetary Laboratory, Tucson, Arizona

W. F. Bottke

Southwest Research Institute, Boulder, Colorado

P. Michel

Observatoire de la Côte d'Azur, Nice, France

and

E. F. Tedesco

TerraSystems Inc., Lee, New Hampshire

Received November 14, 2001; revised April 2, 2002

A recently published model of the Near Earth Object (NEO) orbital–magnitude distribution (Bottke *et al.*, 2002, *Icarus* 156, 399–433.) relies on five intermediate sources for the NEO population: the ν_6 resonance, the 3 : 1 resonance, the outer portion of the main belt (i.e., 2.8–3.5 AU), the Mars-crossing population adjacent to the main belt, and the Jupiter family comet population. The model establishes the relative contribution of these sources to the NEO population. By computing the albedo distribution of the bodies in and/or near each of the five sources, we can deduce the albedo distribution of the NEO population as a function of semimajor axis, eccentricity, and inclination. A problem with this strategy, however, is that we do not know a priori the albedo distribution of main belt asteroids over the same size range as observed NEOs (diameter $D < 10$ km). To overcome this problem, we determined the albedo distribution of large asteroids in and/or near each NEO source region and used these results to deduce the albedo distribution of smaller asteroids in the same regions. This method requires that we make some assumptions about the absolute magnitude distributions of both asteroid families and background asteroids. Our solution was to extrapolate the observed absolute magnitude distributions of the families up to some threshold value H_{thr} , beyond which we assumed that the families' absolute magnitude distributions were background-like.

We found that $H_{\text{thr}} = 14.5$ provides the best match to the color vs heliocentric distance distribution observed by the Sloan Digital Sky

Survey. With this value of H_{thr} our model predicts that the debiased ratio between dark and bright (albedo smaller or larger than 0.089) objects in any *absolute-magnitude-limited* sample of the NEO population is 0.25 ± 0.02 . Once the observational biases are properly taken into account, this agrees very well with the observed C/S ratio (0.165 for $H < 20$). The dark/bright ratio of NEOs increases to 0.87 ± 0.05 if a *size-limited* sample is considered. We estimate that the total number of NEOs larger than a kilometer is 855 ± 110 , which, compared to the total number of NEOs with $H < 18$ (963 ± 120), shows that the usually assumed conversion $H = 18 \Leftrightarrow D = 1$ km slightly overestimates the number of kilometer-size objects.

Combining our orbital distribution model with the new albedo distribution model, and assuming that the density of bright and dark bodies is 2.7 and 1.3 g/cm³, respectively, we estimate that the Earth should undergo a 1000 megaton collision every 63,000 \pm 8000 years. On average, the bodies capable of producing 1000 megaton of impact energy are those with $H < 20.6$. The NEOs discovered so far carry only $18 \pm 2\%$ of this collision probability.

© 2002 Elsevier Science (USA)

Key Words: asteroids; dynamics; composition; spectroscopy.

1. INTRODUCTION

The Near Earth Object (NEO) population is defined as the ensemble of small bodies with perihelion distance $q < 1.3$ AU and

aphelion distance $Q > 0.983$ AU. It is believed that the NEOs with semimajor axis smaller than that of Jupiter are mostly asteroids escaped from the main belt, although some may be extinct cometary nuclei (see Morbidelli *et al.* (2002) for a review). Like the main belt asteroids, the NEOs show a variety of taxonomic classes, which depend on their chemical and physical composition. Some of them (mostly S-class) have high albedos, while others (mostly C-class) have a low reflectivity. In this paper we will categorize the NEOs as “bright” and “dark” bodies, according to their albedo being higher or lower than 0.089, a threshold defined by Tedesco (1994) as the minimum of the bimodal IRAS asteroid albedo histogram, which effectively separates C-class from S-class asteroids. In terms of taxonomic data, following the work of Bus (1999), we consider that the bodies of class A, K, L, O, Q, R, S, V, Xe, and Xk are bright while the bodies of class B, C, D, T, and Xc are dark.

The debiased proportion of dark and bright bodies in the NEO population is not yet known. Of the ~ 1500 NEOs discovered so far, taxonomic data have only been published for ~ 200 . The albedo or taxonomic distribution observed in this small sample cannot be considered representative of the distribution of the whole population because of several biases. One bias that needs to be accounted for is the *phase angle* effect (e.g., Bowell *et al.* 1989, Luu and Jewitt 1989).¹ It can be explained as follows. Let us assume that a bright and a dark body share the same absolute magnitude H . When the dark body is observed at a large phase angle, its visual magnitude V is slightly fainter than the bright body in the same position. Because many NEO discoveries occur at quite large phase angles, this bias may favor the discovery of bright bodies over the dark ones. A second and possibly more important bias is that many dark NEOs should be on orbits with large semimajor axis, because they are supplied mainly by the outer belt and the extinct cometary populations (Bottke *et al.* 2002). Bodies on large- a orbits are generally more difficult to discover than bodies with the same absolute magnitude on orbits with smaller semimajor axis (Jedicke 1996). Therefore, these two biases make the observed dark/bright ratio (called r_{obs} hereafter) smaller than r_H , the true ratio for an *absolute-magnitude-limited* sample of the NEO population. Finally, a third bias should be taken into account if one wants to relate r_{obs} to the true dark/bright ratio for a *size-limited* sample of the NEO population, r_D : dark bodies have a fainter absolute magnitude than bright bodies with the same size and therefore they are much harder to discover.

The first attempt to debias the observed dark/bright ratio of NEOs was made by Luu and Jewitt (1989). For this purpose, they uniformly distributed fake NEOs in a geocentric sphere of radius 1.5 AU. The NEOs were generated following various size distributions, up to a given size. Luu and Jewitt also assumed

that bright NEOs have albedo $p_v = 0.15$ and slope parameter² $G = 0.25$, while dark NEOs have $p = 0.047$ and $G = 0.15$. They considered that a NEO is discovered if its solar elongation is larger than 90° and its visual magnitude is brighter than $V = 15.5$. They found that when 45 NEOs (the number known at that time!) were discovered in their simulation, r_{obs} was reduced with respect to r_D by a factor of 5.6–5.9, depending on the choice of size distribution. From the few taxonomic observations available at the time, Luu and Jewitt estimated that $r_{\text{obs}} \sim 0.1$, which implied $r_D \sim 0.6$. The error bars in this computation were large due to limited statistics, such that a main-belt-like ratio of $r_D \sim 1.5$ could not be ruled out.

A second attempt to determine the dark/bright ratio was made by Shoemaker *et al.* (1990). Taking the phase angle distribution of Earth crossers at their time of discovery, Shoemaker *et al.* (1990) estimated that, on average, the absolute magnitude of C-class asteroids is about 0.16 magnitude brighter than that of S-class asteroids for a given apparent magnitude at the threshold of detection. Therefore, for objects of the same absolute magnitude, the average limiting distance of detection is about 1.07 times greater for S-class objects than for C-class, and the average search volume is 1.24 times greater. These values were used as the bias relating r_{obs} to r_H . Shoemaker *et al.* estimated that $r_{\text{obs}} = 0.35$ (which is different—for some unknown reason—from the estimate made by Luu and Jewitt), which allowed him to calculate a value of $r_H \sim 0.4$. Taking into account the difference in mean albedo between dark and bright bodies, and assuming a reasonable size distribution, these values correspond to $r_D \sim 1.5$.

Determining the debiased dark/bright ratio is not just a matter of curiosity. At present, it is believed that the number of NEOs with $H < 18$ is ~ 1000 and that the cumulative number of objects grows as $10^{0.35H}$ (Rabinowitz *et al.* 2000, Bottke *et al.* 2000, 2002, D’Abramo *et al.* 2001, Stuart 2001). Understanding the distribution of NEO albedos would allow us to convert this H -distribution into a size distribution and ultimately into a mass distribution. This last conversion is now possible thanks to the sharp correlation between bulk density and taxonomic class, revealed by *in situ* measurements of Ida (Belton *et al.* 1995), Mathilda (Yeomans *et al.* 1997), and Eros (Thomas *et al.* 2000) and asteroid satellite observations (Merline *et al.* 1999). [For a review of asteroid bulk density measurements, see Britt *et al.* (2002).] In essence, the bulk density of bright S-class asteroids is ~ 2.7 g/cm³, while that of dark C-class bodies is ~ 1.3 g/cm³. Ultimately, the NEO mass and orbital distributions can be used to compute the collision rate as a function of impact energy on the Earth as well as the other terrestrial planets. These values are essential to our interpretation of the cratering records of the terrestrial planets (a subject of a forthcoming paper). In addition,

² The slope parameter controls how the apparent brightness of the object decays with increasing phase angle. Bodies with large slope parameter are brighter than bodies with small slope parameter, for the same values of absolute magnitude, phase angle, and heliocentric distance. See Eq. (5).

¹ The *phase angle* is the angle between the Sun–object and Earth–object lines, which is equal to 0 if the observation occurs at opposition.

these rates can also be used to assess the hazard to our civilization from NEO impacts (the purpose of this work).

The reason for updating the Luu and Jewitt and Shoemaker *et al.* estimates is twofold. First, a spectacular increase in the number of known NEOs has been achieved over the last 10 years. The current completeness of the $H < 18$ population is about 45%. The biases that relate r_{obs} to r_H and r_D must change with the completeness of the known population, such that they disappear when 100% completeness is reached. Therefore, the values estimated at the end of the 1980s need to be updated so that they can be used to debias the current value of r_{obs} . Second, we now have the potential to do a much more sophisticated job than before, such that we can estimate the albedo distribution not only for the NEO population as a whole but also as a detailed function of the orbital distribution.

Much of the work we present here takes advantage of a model of the NEO orbital-magnitude distribution developed by Bottke *et al.* (2002). This model assumes that the NEO population is currently in steady state and that it is sustained by the continuous influx of material coming from five intermediate sources. Four of these sources are related to the main asteroid belt: (i) the ν_6 resonance population at the inner edge of the belt, (ii) the 3:1 resonance population at 2.5 AU, (iii) the Mars-crossing population with $q > 1.3$ AU and semimajor axis and inclination distributions that mimic those of main belt asteroids, and (iv) the outer belt population with $1.3 < q < 2.4$ AU. The fifth intermediate source is the extinct Jupiter family comet population, which has a trans-Neptunian provenance. The model predicts (with error bars) the NEO population (i.e., number of NEOs as a function of H) in a network of cells in the (a, e, i) space and the relative contributions of the five intermediate sources to the population in each cell. Thus, if we have a reliable estimate of the albedo distribution inside each intermediate source, we can easily compute the albedo distribution in each NEO cell.

To estimate the albedo distribution in each NEO intermediate source, we use the main belt Statistical Asteroid Model (Tedesco *et al.* 2002a). In Section 2 we describe the guidelines along which this model has been constructed and we show that the albedo distribution in the main belt—and therefore also inside the NEO sources—critically depends on one parameter (called H_{thr}). To determine its value, we compare the dark/bright ratio as a function of the heliocentric distance in the main belt with the observations of the Sloan Digital Sky Survey (SDSS) (Ivesić *et al.* 2001). We also compare the resulting dark/bright ratio in our NEO population model with the observed ratio after taking into account the observational biases. Once the parameter's value is fixed, we detail the albedo distribution of the NEO population. In Section 3 we compute the number of NEOs larger than 1 km in diameter in subregions of the NEO space and their dark/bright ratio r_D . We also compare their orbital distribution with that of the NEOs with $H < 18$. In Section 4 we compute the frequency of collisions as a function of their energy. In particular we focus on collisions carrying a kinetic energy larger than 1000 megaton

TNT and compute the frequency of such collisions as a function of the orbital parameters of the impactors.

2. THE NEO ALBEDO DISTRIBUTION MODEL

Observational data on the albedos of main belt asteroids only exist for relatively large bodies. For instance, IRAS observations are limited to asteroids with $H < 13$ and cover a severely incomplete population starting from $H \sim 11$. The NEOs, on the other hand, are almost all fainter than $H = 13$. We cannot say at this time whether the albedo distribution of big asteroids is representative of the albedo distribution of much smaller bodies. While most big asteroids ($D > 50$ km) are primordial objects, the smaller ones are mostly fragments of bigger bodies that have been disrupted over the lifetime of the Solar System. There is no a priori reason to think that the process of fragmentation has preserved the albedo distribution. In particular, since asteroid families become prominent for $H > 12$, and observations suggest that families may contain numerous smaller bodies (e.g., Tanga *et al.* 1999), they have the potential to change the albedo statistics of the overall main belt population all by themselves. Therefore, computing the albedo distribution in the main belt—and in the NEO intermediate sources—requires a careful analysis of the existing data and extensive modeling.

Significant work in this area has already been completed by Tedesco *et al.* (2002a), who constructed a main belt Statistical Asteroid Model (SAM). Next we briefly review the basic ingredients of this model while also discussing its main uncertainties.

2.1. The Statistical Asteroid Model

The SAM has the form of a list of asteroids, with associated orbital elements, absolute magnitude, and albedo. The big asteroids are the real ones, while the small asteroids are mostly synthetic. The synthetic objects have been generated by extrapolating to the corresponding sizes the orbital and physical properties observed among the population of big asteroids. The key principles of the extrapolation procedure are discussed in the following.

The asteroid population has been divided in 18 groups: one for each of the 15 major dynamical families, plus 3 for the “background” population (defined as the population of the asteroids not belonging to any of the 15 considered families, according to the classification of Zappalá *et al.* (1995)). In each group, the observed absolute magnitude distributions have been extrapolated beyond the observational completeness limit. The observed populations have been completed relative to these magnitude distributions by generating the synthetic asteroids. In the three background groups, the semimajor axis, eccentricity, and inclination of the synthetic bodies have been generated according to the observed orbital distribution. In the family groups, a more sophisticated recipe has been followed, because the orbital distribution of the observed family members depends on sizes or, equivalently, on absolute magnitudes (Cellino *et al.* 1999). Small bodies tend to be more dispersed than big bodies. Thus,

the observed magnitude-dependent orbital distribution has been extrapolated up to the absolute magnitudes of the considered synthetic objects, and the synthetic objects' (a, e, i) have been chosen in agreement with these extrapolations.

In each group the characteristic albedo distribution was determined using available radiometric data (about 1500 main belt asteroids) from SIMPS (Tedesco *et al.* 2002b) and the IRTF (Tedesco and Gradie 2002). For the three background groups, only bodies with apparent magnitude at opposition $V < 15.75$ (which constitute a complete sample) have been considered, in order to avoid possible observational biases. The albedos of the synthetic objects (as well as of the real objects for which no albedo data are available) have been randomly generated according to these distributions.

When using the SAM, an important caveat should be kept in mind. Below the completeness limit, the observed magnitude distributions of asteroid families are much steeper than those of the background populations (Tanga *et al.* 1999). Therefore, by extrapolating these distributions to fainter absolute magnitudes, the SAM predicts that the ratio between the numbers of family members and of background objects monotonically and exponentially increases with H (Fig. 1). Because the albedo distribution of family members is different from that of the background objects, this prediction implies that the overall albedo distribution of the main belt in the SAM is absolute magnitude dependent.

It is generally believed, however, that collisional evolution should force the magnitude distribution of asteroid families to

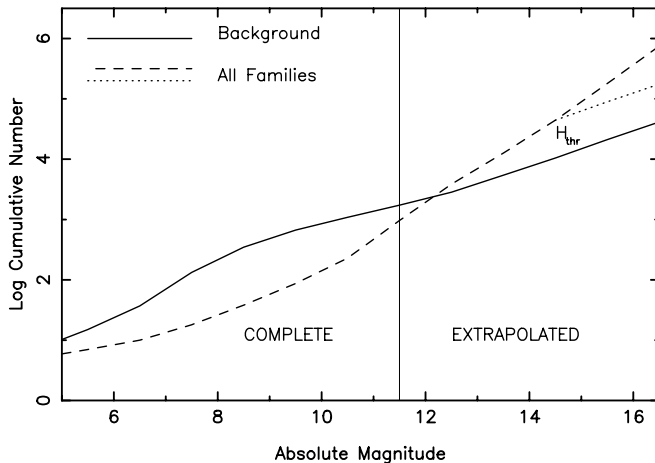


FIG. 1. The cumulative number of background asteroids and family members as a function of the absolute magnitude, according to the SAM model. The bodies that have visual magnitude brighter than 15.75 when they are at opposition at a heliocentric distance equal to their semimajor axis are considered an observationally complete sample. This corresponds to $H \sim 11.5$, as indicated in the plot. Beyond $H = 11.5$ the magnitude distributions of background asteroids and family members are constructed by extrapolation. Because the distribution of family members is steeper, a linear extrapolation results in a ratio between family and background populations that monotonically and exponentially increases with H . However, it is plausible that for H larger than some threshold value H_{thr} the family members reach a collisional equilibrium, background-like, distribution, as sketched in the plot. In this case the ratio between the family and background population would not change beyond H_{thr} .

become shallower and more background-like beyond some threshold magnitude H_{thr} (Marzari *et al.* 1999). If true, the overall albedo distribution should change with H until $H = H_{\text{thr}}$ and stay more-or-less invariant for $H > H_{\text{thr}}$. The problem is that the value of H_{thr} is not known a priori; the most likely circumstance is that H_{thr} varies from family to family as a function of family age (Marzari *et al.* 1999).

To simplify, in this work we assume that there is *one* effective value of H_{thr} , such that the albedo distribution of main belt asteroids with $H > H_{\text{thr}}$ is equal to that given by the SAM for $H < H_{\text{thr}}$. Therefore, since the value of H_{thr} is currently unknown, we construct several SAM- H_{thr} models (i.e., considering only the bodies in the SAM with $H < H_{\text{thr}}$), for a range of values of H_{thr} , and determine which H_{thr} allows the best agreement with the observed dark/bright ratios for the main belt and the NEO populations.

2.2. Dark/Bright Ratio in the Main Belt

The SDSS has recently released data on the dark/bright ratio of main belt asteroids (Ivezić *et al.* 2001). In that study, a color index a^* has been attributed to the observed asteroids through the relationship

$$a^* = 0.89(g^* - r^*) + 0.45(r^* - i^*) - 0.57, \quad (1)$$

where g^* , r^* , and i^* are the measured magnitudes in the g , r , and i bands, respectively. Dark C-class asteroids have $a^* < 0$ and bright S-class asteroids have $a^* > 0$, but unfortunately the color index a^* is not unequivocally related to albedo. In fact the dark D-class asteroids have $a^* > 0$ and the bright E- and M-class bodies have $a^* < 0$. In the 2.1–3.0 AU range, where the D-, E-, and M-class asteroids constitute negligible subpopulations (Gradie and Tedesco 1982), the ratio between the number of bodies with $a^* < 0$ and those with $a^* > 0$ can be considered indicative of the dark/bright ratio of the main belt population. Conversely, beyond 3.0–3.2 AU, where the fraction of D-class becomes significant, the ratio between the number of bodies with $a^* < 0$ and those with $a^* > 0$ is expected to give a lower bound on the real dark/bright ratio.

The black curve in Fig. 2 shows the SDSS survey's measure of the dark fractional component (estimated using the a^* criterion) of an absolute-magnitude-limited sample of the main belt population, as a function of the heliocentric distance. The colored curves show the prediction of the various SAM- H_{thr} models, obtained by attributing to each body a random mean anomaly for the determination of its instantaneous heliocentric distance (as before, a body is considered “dark” if its albedo is smaller than 0.089).

The SAM-15 and SAM-14.5 models are those that best account for the observations. In fact, only the SAM-15 and SAM-14.5 curves repeatedly intersect the SDSS curve, while the SAM-13 and SAM-14 curves are systematically above and the SAM-16 and SAM-17 are systematically below. However, all the models give dark fractions that are larger than the SDSS data for $a > 3.3$ AU, which is presumably due to the presence of numerous D-class asteroids, as explained previously.

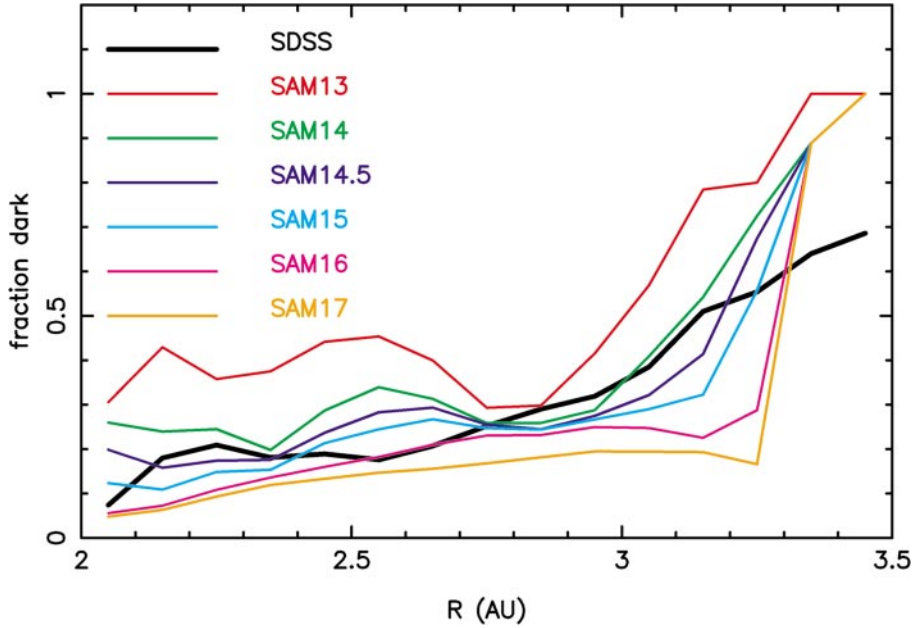


FIG. 2. The fraction of the main belt population that is “dark” as a function of the heliocentric distance. The black curve shows the observational result of the SDSS survey, where the “dark” bodies are identified as those with color index $a^* < 0$ (mostly C-class). The curves labeled SAM H_{thr} are those obtained from the SAM model with the restriction $H < H_{\text{thr}}$ and identifying as “dark” the bodies with albedo smaller than 0.089.

The similarity between the SDSS curve and the SAM-14.5 and SAM-15 curves gives us confidence that the $H_{\text{thr}} \sim 14.5$ – 15 is a reasonable preliminary choice to input into our albedo distribution model. Two additional arguments concur in this direction: (i) if the steep magnitude distribution of asteroid families continued beyond $H_{\text{thr}} \sim 15$, the predicted total number of main belt objects would exceed that estimated by Jedicke and Metcalfe (1998) and by Ivezić *et al.* (2001) by debiasing detections from the Spacewatch survey; (ii) according to the SDSS survey’s results and Jedicke and Metcalfe (1998), the cumulative magnitude distribution of the main belt population follows a broken law, with a break point (from steeper to shallower) at $H \sim 15$.

Notice that, according to our model, a value $H_{\text{thr}} \lesssim 15$ implies that the NEOs (which are essentially all fainter than this threshold) have an albedo distribution that is absolute magnitude independent.

2.3. The Construction of the NEO Albedo Model

To compute the albedo distribution of the NEOs coming from each asteroidal intermediate source, we compile statistics on the SAM- H_{thr} populations in four regions defined as follows:

- ν_6 source: a band 0.05-AU wide on the right-hand side of the curve that denotes the location of the ν_6 resonance in the (a, i) plane (see Fig. 2 of Morbidelli and Gladman (1998));
- 3:1 source: the region with $2.48 - 0.075e < a < 2.52 + 0.10e$ AU;
- IMC source: the region with $2.1 < a < 2.8$ AU and $q < 1.8$ AU;
- OB source: the region with $a > 2.8$ AU and $q < 2.4$ AU.

In all cases, the regions are delimited also by the conditions $q > 1.3$ AU and $i < 16^\circ$. The choice of these regions is the result of a compromise between the desire of being consistent with the definition of the NEO intermediate sources given in Bottke *et al.* (2000, 2002) and the necessity of working on sufficiently large regions that include a statistically significant number of bodies from the SAM- H_{thr} populations.

In each region, we categorize the asteroids in the four albedo classes defined by Tedesco *et al.* (2002a) and listed in Table 1 (i.e., high, moderate, intermediate, low). In each albedo class we assume that all bodies have albedo equal to the mean value of the class. Thus, the albedo distribution in each of our NEO source regions is reduced to the relative proportion among the populations in the albedo classes and can be represented by four coefficients, $d_{\text{albedo class}}^{\text{NEO source}}$, whose sum is equal to 1. In addition to the four albedo classes just defined, we also introduce a *Com* class exclusively for the cometary source of NEOs. It is therefore intended that $d_{\text{Com}}^{\text{NEO source}} = 0$ for the asteroidal sources, while $d_{\text{Com}}^{\text{JFC}} = 1$.

TABLE 1
Definition of the Albedo Classes Used in Our Model

Class	Albedo range	Mean albedo
<i>Hig</i>	0.355–0.526	0.462
<i>Mod</i>	0.112–0.355	0.197
<i>Int</i>	0.089–0.112	0.099
<i>Low</i>	0.020–0.089	0.055
<i>Com</i>	??	0.04

We now have all the ingredients to construct a NEO albedo model. The Bottke *et al.* (2002) model estimates

- the total number of NEOs with $H < 18$: $N(H < 18)$;
- the H -distribution of NEOs: $N(H < H_{\text{lim}}) = N(H < 18) \times 10^{0.35(H_{\text{lim}}-18)}$;
- the fraction of the total NEO population contained in each (a, e, i) cell of the NEO space: $R(a, e, i)$; and
- the fraction of the population in each cell that comes from each of the five intermediate sources: $c_{\text{NEO source}}(a, e, i)$.

Therefore, the fraction of the NEO population in a cell that belongs to a given albedo class is simply

$$f_{\text{albedo class}}(a, e, i) = \sum_{\text{NEO source}} c_{\text{NEO source}}(a, e, i) d_{\text{albedo class}}^{\text{NEO source}}, \quad (2)$$

where the sum is made over the five NEO sources. The fraction of the total NEO population that belongs to a given albedo class is then

$$F_{\text{albedo class}} = \sum_{(a,e,i)} R(a, e, i) f_{\text{albedo class}}(a, e, i), \quad (3)$$

where the sum is done over all cells in the NEO space. Finally, the dark/bright ratio of the NEO population is, for an absolute-magnitude-limited sample,

$$r_H = (F_{\text{Com}} + F_{\text{Low}})/(F_{\text{Int}} + F_{\text{Mod}} + F_{\text{Hig}}). \quad (4)$$

Table 2 gives the dark/bright ratio r_H obtained with the various SAM- H_{thr} models that we have considered. Also reported is the dark/bright ratio computed for the NEO subpopulation restricted to the region with $a < 2.5$ AU, a threshold that is often used to separate the the NEOs that predominantly come from the inner belt from those that come from the outer belt. As one sees, r_H decreases monotonically with increasing H_{thr} ; this is because the relative proportion of family members in the main belt

population increases and because most families predominantly contribute to the bright classes *Int*, *Mod*, and *Hig*. Notice also that the dark/bright ratio for NEOs with $a < 2.5$ AU is smaller than the one for the whole NEO population, indicating that most of dark NEOs reside on orbits with $a > 2.5$ AU.

The next step before comparing r_H with the observed ratio is the evaluation of our observational biases.

2.4. A NEO Survey Simulator

Jedicke *et al.* (2002) have designed a survey simulator inspired by the known characteristics of the LINEAR survey. In particular, the survey simulator covers an area of sky comparable to the average monthly coverage of LINEAR (as given on <http://asteroid.lowell.edu/cgi-bin/koehn/coverage>) in 14 days around new Moon. Its detection efficiency is 100% for NEOs with visual magnitude $V < 17.75$ and linearly decays to 0% in the next 1.5 magnitudes. In addition, only bodies with an apparent rate of motion faster than 0.3 deg/day are considered to be detected. Despite being specifically designed for LINEAR, the survey simulator does a good job of reproducing the overall performance of all NEO surveys that have contributed to the observed NEO population so far. In fact, Fig. 3 shows off the excellent agreement between (1) the known distribution of 469 NEO with $H \leq 18$ (dotted line) as of 15 March 2001 and (2) the distribution of the synthetic NEOs generated according to the Bottke *et al.* (2002) model (solid line) and detected by the survey simulator (points with 1σ error bars). We can therefore take advantage of this survey simulator to compute the expected observed (i.e., biased) dark/bright ratio for each of the NEO albedo distribution models.

For this purpose, we first need to incorporate the albedo-dependent phase angle effect, briefly discussed in the introduction. The IAU recommended formula for computing the visual magnitude V of a body with phase angle $\alpha < 120^\circ$ is (Bowell *et al.* 1989)

$$V = 5 \log(r\Delta) + H - 2.5 \log[(1 - G)\phi_1 + G\phi_2], \quad (5)$$

where r and Δ are, respectively, the heliocentric and geocentric distances, H is the absolute magnitude, G is called the slope parameter, and ϕ_1 and ϕ_2 are quantities that depend on α through the relationships

$$\begin{aligned} \phi_1 &= \exp\{-[3.33 \tan(\alpha/2)]^{0.63}\}, \\ \phi_2 &= \exp\{-[1.87 \tan(\alpha/2)]^{1.22}\}. \end{aligned} \quad (6)$$

Formula (5) implies that the visual magnitude of an object becomes fainter as the phase angle increases. The albedo-dependent phase angle effect arises because the slope parameter is smaller for low-albedo objects than for high-albedo ones. As a consequence, the rate at which V becomes fainter with increasing α is higher for low- G objects. In other words, given H and $\alpha \neq 0$, a low- G object has a fainter visual magnitude than

TABLE 2
Dark/Bright Ratios for Various SAM- H_{thr} Models

H_{thr}	r_H (all a)	r_{obs} ($H < 18$)	r_{obs} ($H < 20$)	r_H ($a < 2.5$)	r_{obs} ($H < 18$)	r_{obs} ($H < 20$)
13	0.56	0.44	0.42	0.42	0.39	0.36
14	0.38	0.30	0.28	0.26	0.25	0.24
14.5	0.25	0.18	0.17	0.14	0.14	0.13
15	0.23	0.17	0.15	0.13	0.12	0.12
16	0.17	0.12	0.11	0.08	0.08	0.07
17	0.16	0.11	0.10	0.07	0.07	0.07

Note. The numbers corresponding to our preferred model are reported in boldface. The biased ratios r_{obs} are measured on the objects detected by the NEO survey simulator when 45% completeness on the $H < 18$ population is achieved.

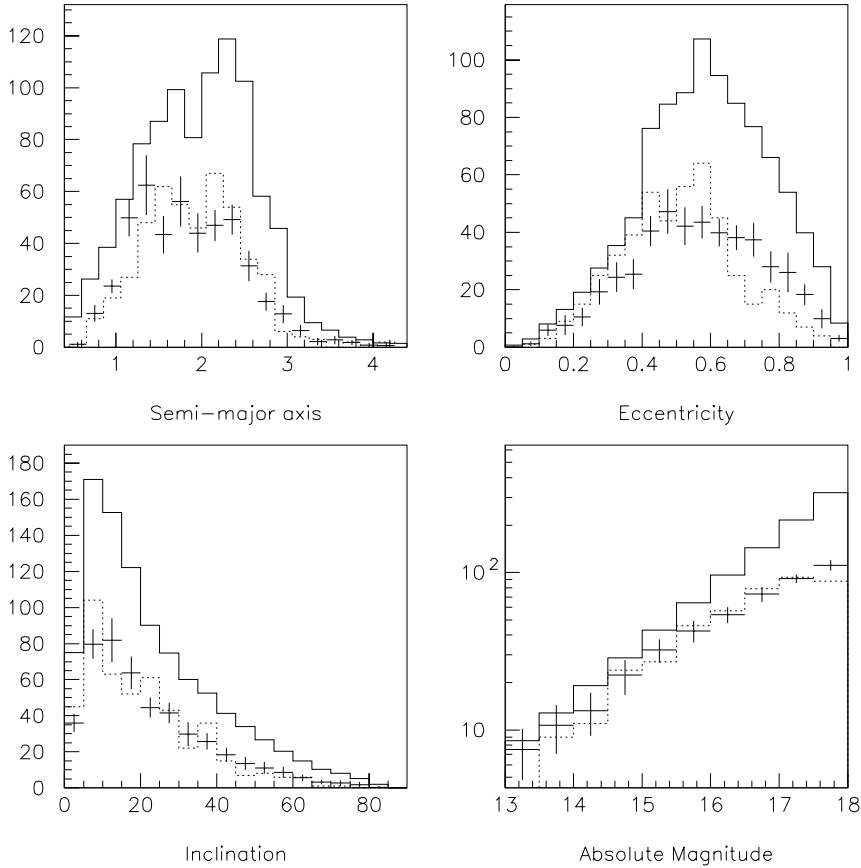


FIG. 3. The solid line represents the (a, e, i, H) distribution of NEOs according to Bottke *et al.*'s (2002) model. The points with (1σ) error bars give the distribution of the NEOs detected by the survey simulator. The dotted line represents the distribution of the NEOs with $H < 18$ discovered as of 15 March 2001.

a high- G object. To simulate the phase angle effect we assign

- $G = 0.13$ to the *Com* class,
- $G = 0.15$ to the *Low* class,
- $G = 0.18$ to the *Int* class,
- $G = 0.25$ to the *Mod* class, and
- $G = 0.40$ to the *Hig* class.

These numbers have been obtained using a linear least-squares fit to the albedos versus measured G values as given in the SIMPS database (Tedesco *et al.* 2002b).

For each NEO albedo distribution model listed in Table 2, we generate 10 sets of 4886 synthetic NEOs with $H < 20$ (the number predicted in Bottke *et al.* (2002)), and we run on each set the survey simulator until 45% completeness is achieved on the population with $H < 18$. Accordingly, the observed NEO population with $H < 20$ is far less complete (19.5%). The dark/bright ratio of the detected NEOs is computed separately for the NEOs with $H < 18$ and $H < 20$, and also for the NEO subpopulation with $a < 2.5$ AU.

The results, averaged over the simulations corresponding to the 10 sets generated from the same NEO model, are listed in Table 2. Notice that for the overall NEO population, the dark/bright ratio of the detected bodies (r_{obs}) is always smaller than the

true ratio r_H . Thus a bias in favor of the discovery of bright bodies really exists. This bias is slightly more severe for the $H < 20$ population than for the $H < 18$ population, which shows that the bias gradually reduces with increasing observational completeness of the considered population, as expected. Conversely, the bias on the dark/bright ratio is almost nonexistent for the NEOs with $H < 18$ and $a < 2.5$ AU (compare r_{obs} to r_H in the fifth and sixth columns). This means that for the overall $H < 18$ NEOs, the bias is mostly because dark bodies predominantly reside on orbits with $a > 2.5$ AU.

2.5. Dark/Bright Ratio for NEOs

At this point we can compare the simulated dark/bright ratios in Table 2 to the observed dark/bright ratio for real NEOs and check which SAM- H_{thr} model allows the best agreement with the data.

We first update the list of NEOs with known albedo or taxonomic class. Our sources are:

- the SIMPS data set, a re-elaboration of IRAS observations (Tedesco *et al.* 2002b), which provides direct information on the albedos;
- unpublished IRTF data from Tedesco and Gradie (2002), which provide direct information on the albedos;

- the appendix of Lupishko and DiMartino (1998), which provides a list of taxonomic classes (we discard the bodies for which an albedo is assumed without a taxonomic classification); and
- the recently released SMASS2 data (Bus and Binzel 1998), which also provide a list of taxonomic classes.

The taxonomic classes that are categorized as “bright” or “dark” are given at the beginning of the introduction of this paper. If a NEO has both a direct albedo measurement and a taxonomic classification, we always refer to the albedo measurement.

In total, we have collected data on 183 NEOs with $H < 20$. The top panels of Fig. 4 show the dark/bright ratio r_{obs} computed for NEOs grouped in one-magnitude-wide bins. The dashed histogram gives the number of data in each bin. Also shown are the 1σ and 2σ error bars for the computed ratios. The error bars are computed with a simple Monte Carlo code. Given the number N of bodies on which r_{obs} is measured, we fix a “true” ratio r_* and we randomly generate 1000 sets of N data that are categorized as “dark” or “bright” according to the probability distribution

imposed by the r_* ratio. If the resulting dark/bright ratio r_{MC} is such that $r_* < r_{\text{obs}} < r_{\text{MC}}$ or $r_{\text{MC}} < r_{\text{obs}} < r_*$ for more than 32% of the generated sets, we say that the ratio r_* belongs to the 1σ error bar of r_{obs} . Analogously, if the above inequalities occur for more than 5% of the sets, we say that the ratio r_* belongs to the 2σ error bar of r_{obs} .

The data puzzle us, for two reasons. First, the observed dark/bright ratio fluctuates wildly from one magnitude bin to the other. These fluctuations seem to be inconsistent with a constant dark/bright ratio at the 1σ level (the corresponding error bars do not overlap), while they might be consistent with a constant ratio at the 2σ level (the corresponding error bars marginally overlap). Second, the data give the visual impression that the dark/bright ratio has an overall trend to increase with H . In contrast, we do not see any real reason for significant fluctuations in the dark/bright ratio (apart from random sampling) and, if any, we would expect exactly the opposite overall trend! In fact, we have argued previously that the observational bias should tend to slightly *decrease* the dark/bright ratio for bodies with larger H . Also, the SAM predicts that the dark/bright ratio *decreases* with increasing H ,

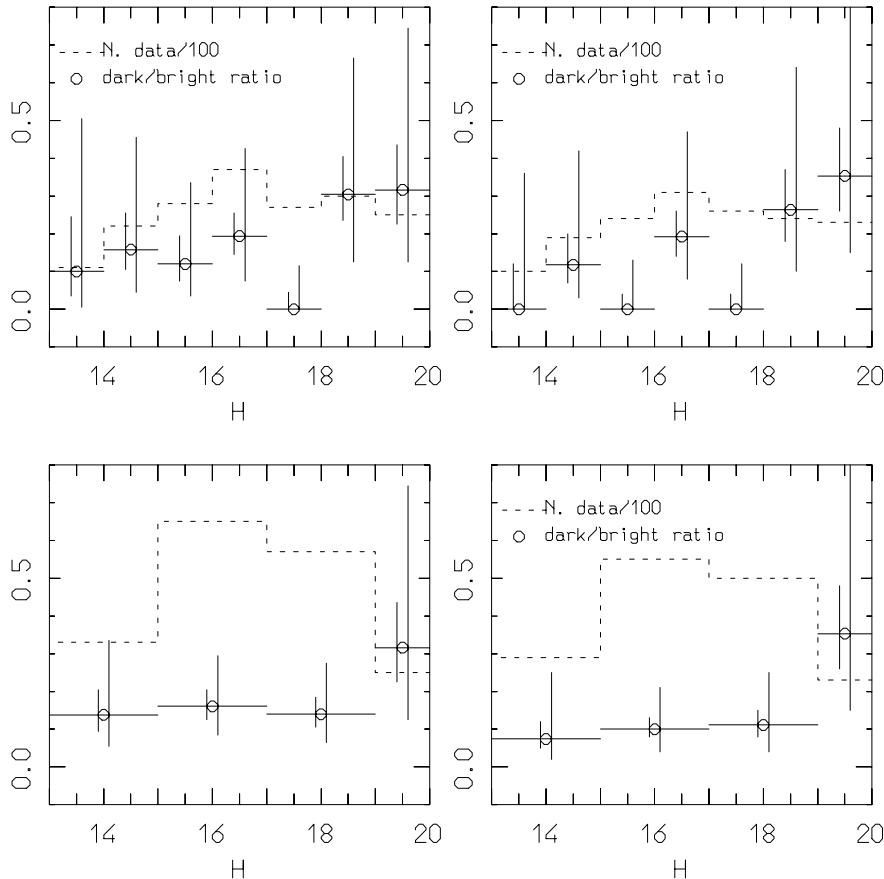


FIG. 4. Top panels: The open dots show the dark/bright ratios computed for NEOs grouped in one-magnitude-wide bins. The horizontal solid lines show the extent of each magnitude bin over which the ratio is computed, while the vertical solid lines on both sides of each open dot denote the 1σ and 2σ error bars. The dashed histogram shows the number of data in each magnitude bin, divided by 100 for scale reasons. The left panel concerns NEOs without restrictions on the orbital elements, while the right panel includes only NEOs with $a < 2.5$ AU. Bottom panels: the same as the top panels, but the NEOs with $13 < H < 19$ are grouped in two-magnitude-wide bins.

TABLE 3
Albedo Distributions According to the SAM-14.5 Model

Source	<i>Com</i>	<i>Low</i>	<i>Int</i>	<i>Mod</i>	<i>Hig</i>
v_6	0.00	0.07	0.05	0.74	0.14
3 : 1	0.00	0.10	0.04	0.79	0.07
IMC	0.00	0.21	0.06	0.63	0.10
OB	0.00	0.47	0.11	0.39	0.03
JFC	1.00	0.00	0.00	0.00	0.00
NEO	0.06	0.14	0.05	0.65	0.10

Note. The first five lines show the relative proportion in the *Com*, *Low*, *Int*, *Mod*, and *Hig* albedo groups, for each source region of the NEO population. The last line shows the resulting overall albedo distribution of the NEO population.

so that no choice of H_{thr} in our models could reproduce the apparent trend. Our expectation for a quasi-constant dark/bright ratio is reinforced by the fact that, if we collect the NEO data in two-magnitude-wide bins, as in the bottom panels of Fig. 4, the resulting ratios in the 13–15, 15–17, and 17–19 bins are almost the same, and the only “anomaly” in the dark/bright ratio appears for NEOs with $H > 19$ (only 36 bodies in our database).

For these reasons, we think that the available data do not yet provide convincing evidence that the dark/bright ratio of NEOs is magnitude dependent, and we use the entire collection of NEOs with $H < 20$ to compute the observed ratio. We obtain $r_{\text{obs}} = 0.165 \pm 0.015$ (1σ) for the NEOs without restriction on the semimajor axis and $r_{\text{obs}} = 0.130 \pm 0.010$ (1σ) for the NEOs with $a < 2.5$ AU. These numbers are in very good agreement with the r_{obs} values reported in Table 2 for our model with $H_{\text{thr}} = 14.5$, which reinforce our preliminary choice of H_{thr} , made in Section 2.2 from the visual comparison with the SDSS data on the color distribution of main belt asteroids. Therefore, we use $H_{\text{thr}} = 14.5$ for the generation of our “best” NEO albedo distribution model. The resulting albedo distributions in the NEO source regions and in the NEO population are reported in Table 3. All numbers are given for absolute-magnitude-limited populations.

The 1σ error bar on the observed dark/bright ratio translates into an uncertainty on the value of H_{thr} ranging from 14.25 to 15. These values will be used to compute the error bars on the quantities (number of NEOs larger than 1 km, frequency of impacts, etc.) estimated in the following sections. In principle, in the computation of these error bars we should also take into account the uncertainties in the Bottke *et al.* NEO model, namely, the uncertainties on the parameters α_{IS} that control the relative importance of the NEO sources (see Bottke *et al.* 2000, 2002). However, the α_{IS} and H_{thr} should not be treated as independent. In fact, for each set of α_{IS} within the error bars of the Bottke *et al.* model we would determine a slightly different interval of values of H_{thr} to obtain the *same* interval of NEO dark/bright ratios (corresponding to the observed ratio and its error bar). Hence, by construction, the uncertainty on the α_{IS} does not increase the uncertainty on the resulting NEO dark/bright ratio. Supposing that this is almost true for the other quantities of interest as well,

an approximate but effective way to compute the error bars on the resulting model is to fix the α_{IS} (for instance, equal to the best-fit values determined by Bottke *et al.* (2002)) and let H_{thr} range over its corresponding interval of uncertainty.

3. FROM MAGNITUDES TO DIAMETERS

Armed with the NEO albedo distribution model, we can now compute the number of bodies larger than a given size D in each (a, e, i) cell of the model. For each albedo class, the absolute magnitude corresponding to a size D is computed as

$$H_{\text{albedo class}}^D = 2.5(6.244 - \log p_v^{\text{class}} - 2\log D), \quad (7)$$

where p_v^{class} is the mean albedo of the considered class. Thus, the total number of NEOs larger than D_{min} in a (a, e, i) cell is

$$N(D > D_{\text{min}})(a, e, i) = R(a, e, i) \sum_{\text{albedo class}} f_{\text{albedo class}} N(H < H_{\text{albedo class}}^{D_{\text{min}}}), \quad (8)$$

where the sum is done on the five albedo classes,

$$N(H < H_{\text{albedo class}}^{D_{\text{min}}}) = N(H < 18) \times 10^{0.35(H_{\text{albedo class}}^{D_{\text{min}}} - 18)}, \quad (9)$$

and $f_{\text{albedo class}}$ is defined in (2).

Finally, the dark/bright ratio of the NEOs larger than D_{min} is

$$r_D = \frac{F_{\text{Com}} \times 10^{0.35H_{\text{Com}}^{D_{\text{min}}}} + F_{\text{Low}} \times 10^{0.35H_{\text{Low}}^{D_{\text{min}}}}}{F_{\text{Int}} \times 10^{0.35H_{\text{Int}}^{D_{\text{min}}}} + F_{\text{Mod}} \times 10^{0.35H_{\text{Mod}}^{D_{\text{min}}}} + F_{\text{Hig}} \times 10^{0.35H_{\text{Hig}}^{D_{\text{min}}}}}, \quad (10)$$

where $F_{\text{albedo class}}$ is defined in (3). By substitution of (7) into (10) it is easy to check that r_D is independent of D_{min} .

Table 4 reports the total number of NEOs larger than 1 km in diameter and their dark/bright ratio r_D obtained from our preferred albedo model ($H_{\text{thr}} = 14.5$). The respective numbers for the subpopulation with $a < 2.5$ AU are also shown. The table

TABLE 4
Number of NEOs Estimated to Be Larger Than 1 km in Diameter and Their True Dark/Bright Ratio r_D for Each SAM- H_{thr} Model

H_{thr}	$N(>1\text{km})$ (all a)	r_D	$N(>1\text{km})$ ($a < 2.5$)	r_D
13	1058	1.75	748	1.24
14	955	1.24	660	0.80
14.5	855	0.87	570	0.45
15	834	0.82	555	0.42
16	766	0.64	500	0.27
17	765	0.57	504	0.23

Note. The numbers corresponding to our preferred model are reported in bold face.

also reports the numbers that would be obtained from the models corresponding to different values of H_{thr} .

Assuming that the total number of NEOs with $H < 18$ is 963 (Bottke *et al.* 2002), our preferred model predicts the existence of 855 bodies larger than 1 km in diameter; the uncertainty on the value of H_{thr} (from 14.25 to 15) translates into an uncertainty of ± 20 bodies on the latter estimate. This shows that the usually assumed conversion $H = 18 \Leftrightarrow D = 1$ km slightly overestimates the total number of kilometer-size objects; we compute that, on average, the correspondence should be $H = 17.85 \pm 0.03 \Leftrightarrow D = 1$ km. Similarly, the uncertainty of H_{thr} gives an uncertainty on the ratios r_H and r_D of ± 0.02 and ± 0.05 respectively. Assuming that the uncertainty on the total number of NEOs with $H < 18$ is ± 120 (Bottke *et al.* 2002), we estimate that total uncertainty on the number of NEOs larger than 1 km is ± 110 .

Figure 5 compares the debiased orbital distributions of the NEOs with $H < 18$ and of those with $D > 1$ km. Because the dark NEOs come mainly from the outer belt or are dormant cometary nuclei, their orbits typically have large semimajor axis. Therefore, the NEOs with $D > 1$ km outnumber those with $H < 18$ for $a > 2.5$ AU, while the opposite is true for $a < 2.5$ AU.

In the eccentricity distribution, the bodies with $H < 18$ outnumber those with $D > 1$ km for $e < 0.6$, a consequence of the fact that most of the NEOs (and all the Earth-crossers) less eccentric than this threshold have $a < 2.5$ AU. The inclination distributions of $H < 18$ and $D > 1$ km NEOs are essentially identical.

4. EARTH COLLISION HAZARDS

In this section, we apply our results from the previous sections to estimate the potential hazard to the Earth from Earth-crossing NEOs. To assess the threat, we must first develop a metric to characterize the danger. A report delivered to NASA (and ultimately the U.S. Congress; Morrison 1992) suggested that an asteroid or a comet should be considered dangerous to human civilization if it could produce upon impact the energy equivalent to 50,000 megaton TNT (or more). On average, it was estimated that a 1-km NEO striking the Earth was capable of producing such energies (assuming a 50 : 50 mix of bright and dark NEOs, 1-km bodies roughly translate into $H < 18$ bodies). More recently, the report of the UK Taskforce on NEO

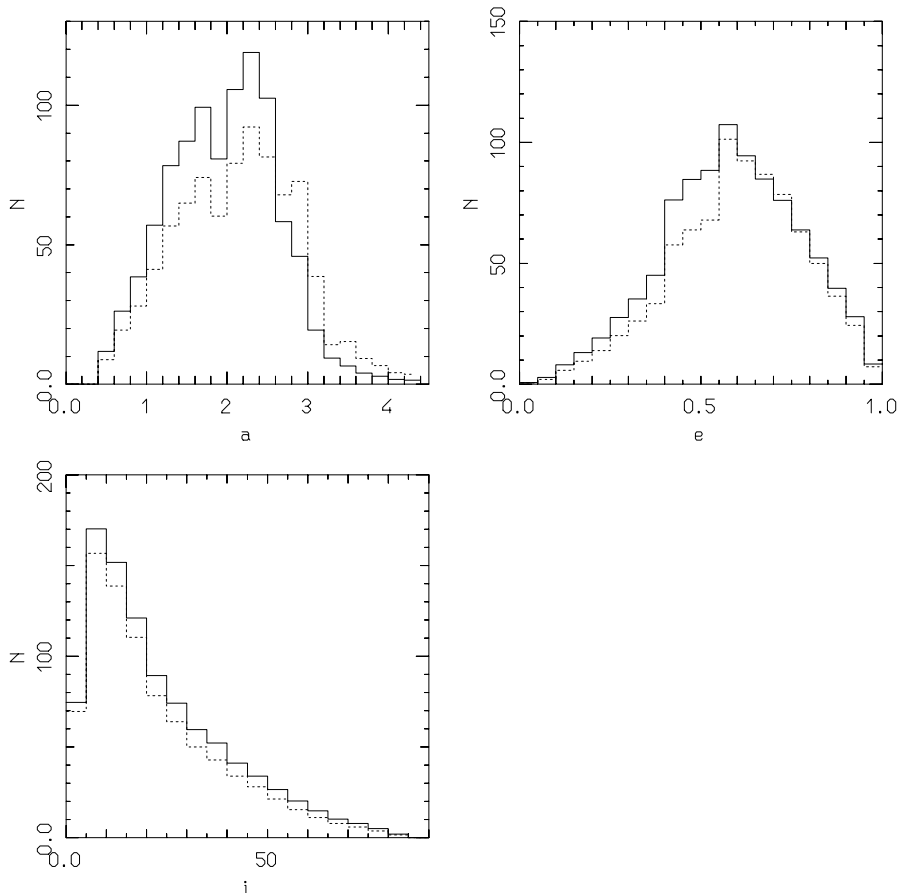


FIG. 5. Debiased (a, e, i) distribution of NEOs with $H < 18$ (solid histograms) and $D > 1$ km (dashed histograms). The first distribution is that given in Bottke *et al.* (2002), while the latter is deduced from the former by using our SAM-14.5 albedo distribution model.

Hazards (NEO Taskforce 2000) stressed that impact energies of ~ 1000 megaton should also be considered a threat to human life, since they could potentially produce large-scale regional damage.

Using our NEO orbital–magnitude–albedo model, we can estimate (1) the frequency of collisions carrying an impact energy larger than a reference threshold and (2) the orbital distribution of the impactors. The kinetic energy of a projectile in units of megaton TNT (MT) is given by

$$E = 62.5\rho D^3 v^2, \quad (11)$$

where ρ is the bulk density of the projectile in g/cm^3 , D is the diameter of the projectile in kilometers, and v is the impact velocity in km/s. Measurements of the asteroid bulk densities (Britt *et al.* 2002) show a sharp correlation between bulk density and asteroid taxonomic class. Based on these results, we assume that C-class bodies have $\rho \sim 1.3 \text{ g/cm}^3$ while S-class bodies have $\rho \sim 2.7 \text{ g/cm}^3$. Therefore, in our model we assume that the former density is typical of the *Com* and *Low* albedo classes while the latter is typical of the *Int*, *Med*, and *Hig* classes. In making this approximation, we ignore the fact that metallic asteroids have much larger densities, and comets possibly have lower densities than carbonaceous asteroids. We do not consider this to be a serious limitation of our model, because comets account for only $\sim 5\%$ of the NEO population and iron objects do not appear to constitute a significant fraction at all (only 2 NEOs among the 183 in our database belong to the M-class, and some M-class asteroids do not appear to be metallic; Rivkin *et al.* 2002). Nevertheless, we have also tried different values for the bulk density, as low as 0.3 g/cm^3 for the bodies of the *Com* class, and as high as 5 g/cm^3 for the bodies in the *Hig* class, never getting differences larger than $\pm 3\%$ in the resulting overall frequency of impacts of given energy on Earth.

For each (a, e, i) cell in the NEO space, we first compute the mean unperturbed encounter velocity with the Earth, $v_\infty(a, e, i)$, using the formulas given in Bottke *et al.* (1994a). The mean impact velocity is then computed taking into account the Earth's induced gravitational acceleration, namely,

$$v_{\text{imp}}(a, e, i) = \sqrt{v_\infty(a, e, i)^2 + v_E^2}, \quad (12)$$

where $v_E = 11.2 \text{ km/s}$ is the Earth's escape velocity. Using (12) in (11) and the albedo-dependent density discussed previously, we compute for each albedo class and (a, e, i) cell the minimum diameter of an object capable of producing a given impact energy upon collision with the Earth. The diameter is converted into a limiting absolute magnitude using (7), and the total number of objects brighter than that magnitude is computed in each cell using (8).

The last step is to compute the number of expected collisions between Earth and the dangerous objects in each cell. For this purpose, we multiply the number of dangerous objects in each cell with the mean collision probability characterizing the

population in that cell. The latter is computed using an algorithm described by Bottke *et al.* (1994a,b), which is an updated version of similar models described by Öpik (1951), Wetherill (1967), and Greenberg (1982). This algorithm assumes that the values of the orbital angles (mean anomaly, longitude of node, argument of perihelion) of the Earth and the NEOs are random, and it also takes into account the gravitational attraction exerted by the Earth, which enhances the collision probability by a so-called gravitational focusing factor. Conversely, it cannot take into account the phenomena of resonance protection (Milani and Baccili 1998) and resonance returns (Milani *et al.* 1999), which respectively reduce and enhance the collision probability of specific objects with respect to that of a population with the same values of a , e , and i and a uniform distribution of the angular elements.

Figure 6 shows the results for collisions with energy larger than 1000 MT (solid histograms). On average, the absolute magnitude of bodies capable of producing 1000 MT of impact energy is $H = 20.6$, although occasionally bodies up to $H = 23$ can produce such an impact energy. The discovery of these bodies—albeit important—goes well beyond the stated Spaceguard goal. The interval between 1000 MT impacts on the Earth is $\sim 63,000$ years. Most of the danger is carried by NEOs with $a < 2 \text{ AU}$. Bodies with large semimajor axes, despite being more numerous, represent only a minor risk, because (i) they have a lower collision probability with the Earth and (ii) they are mostly low-density bodies. Also, a relative majority of impacts are expected from objects with $i < 5^\circ$, despite the fact that the Bottke *et al.* (2002) model does not show many objects with this kind of inclination compared to the number with $i > 5$ degrees (compare the bottom panel of Fig. 6 to that of Fig. 5). This is due to the enhanced individual collision probability of low-inclination objects.

Our predicted interval between 1000 MT impacts on Earth appears to be roughly a factor of 4 larger (or, equivalently, the impact rate is 4 times smaller) than that predicted by Morrison *et al.* (1994), who based their results on those found by Shoemaker (1983). Though sorting out the exact reason for this difference is beyond the scope of this paper, we believe we understand the main issues. To compute the 1000-MT impact frequency on Earth, Shoemaker (1983) needed to estimate several poorly known components (i.e., the number of impactors capable of producing a 1000-MT impact, the fraction of bright/dark objects in the NEO population, the impact frequency of NEOs striking the Earth, the flux of cometary objects striking the Earth, etc.). In comparing these components to our estimates, two particular values stand out: (i) to calibrate his values, Shoemaker assumed that the population of $H < 18$ bodies capable of striking the Earth is ~ 1300 , nearly a factor of 2 larger than predicted by the Bottke *et al.* (2002) model; (ii) to estimate the population of bodies capable of producing 1000-MT blasts on the Earth, Shoemaker converted lunar craters into projectiles using, among other estimates, an approximate crater scaling relationship. We believe the uncertainty in this relationship is such that even a

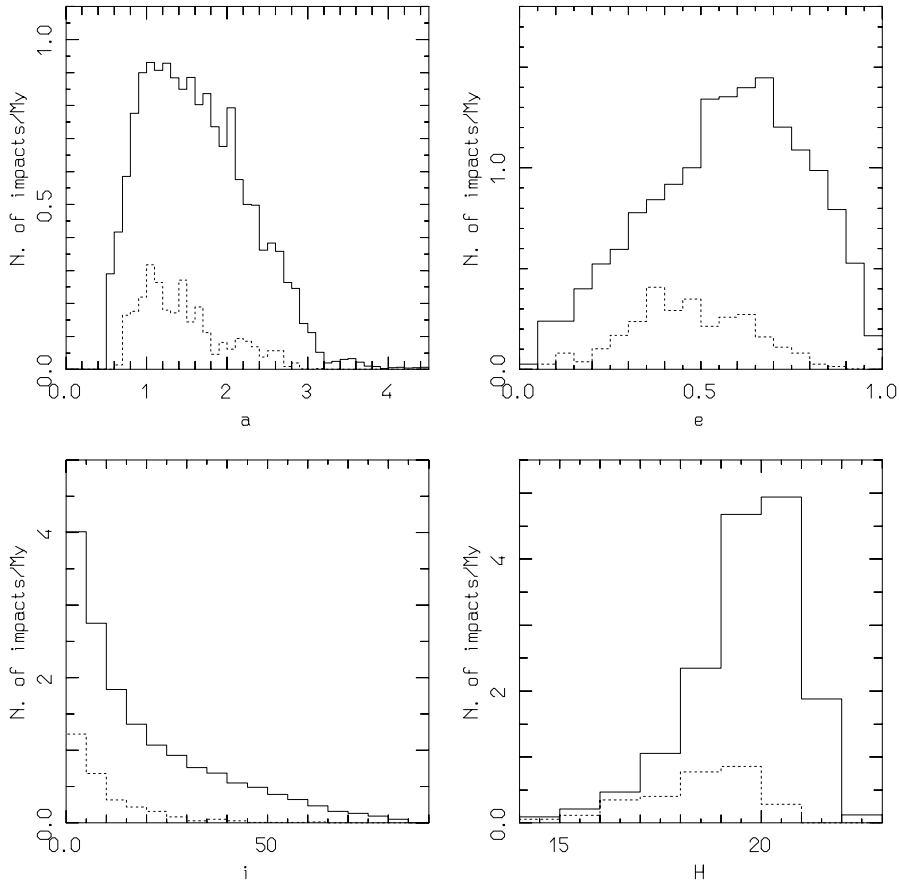


FIG. 6. The expected number of collisions carrying an impact energy larger than 1000 megaton TNT, as a function of the impactors’ orbital parameters and absolute magnitude (solid histogram). For comparison, the dashed histogram shows the number of collisions expected from the known NEO population. The completeness of the known population, measured relative to the total collision probability, is only $\sim 18\%$.

small tweaking of values could easily introduce another factor of 2 into the results. We leave a more thorough investigation of this topic for the future.

In Fig. 6, the dashed histogram shows the number of impacts with energy larger than 1000 MT, expected from the population of the NEOs discovered so far. The histogram has been computed with the following recipe:

- An albedo has been randomly attributed to all known NEOs, according to the albedo distribution in their respective (a, e, i) cells.
- With the attributed albedos, each NEO absolute magnitude has been converted into size and mass (assuming again $\rho = 1.3 \text{ g/cm}^3$ if the albedo is smaller than 0.089 and $\rho = 2.7 \text{ g/cm}^3$ otherwise).
- For each NEO, the impact energy is computed using the mean impact velocity that characterizes its (a, e, i) cell; only NEOs with impact energy larger than 1000 MT are retained.
- The number of the NEOs retained in each cell is multiplied by the cell’s mean collision probability.

Cumulatively, the collision probability of the known NEOs is only 18% of the total estimated collision rate. This value means

that there is an 82% probability that we have not yet discovered the NEO that could cause the next catastrophe.

In Table 5 we report the average time interval between collisions for various energy values and the current completeness of the corresponding projectile population. The error bars on the frequency of impacts and on the completeness are computed from the relative uncertainty on the population of objects of a given size ($\pm 13\%$). The error bars on the average absolute magnitude and diameter of the objects corresponding to the

TABLE 5
Threshold Energy for “Dangerous” Impacts, Mean Interval between Successive Impacts, Current Completeness of the Impactor Population, and Absolute Magnitude and Diameter of the NEOs That Produce the Impact

Energy (megaton TNT)	Average interval (years)	Completeness	H	D (m)
1000	$63,000 \pm 8000$	0.18 ± 0.02	20.63 ± 0.03	277 ± 7
10,000	$241,000 \pm 30,000$	0.37 ± 0.05	18.97 ± 0.03	597 ± 15
100,000	$925,000 \pm 121,000$	0.49 ± 0.06	17.30 ± 0.03	1287 ± 33

Note. Error bars are computed as mentioned in the text.

selected impact energy are computed from the uncertainty on the parameter H_{thr} , characterizing the albedo distribution model.

We caution that our NEO model does not incorporate the population of dormant comets of Oort cloud provenance (while it does include the population of dormant Jupiter family comets). However, this is not a serious limitation, because a recent work by Levison *et al.* (2002) shows that dormant long-period and Halley-type comets with $H < 18$ should collide with the Earth only every 370 and 780 Myr, respectively. These collision intervals are very long compared to the 0.5-Myr, period typical of $H < 18$ NEOs of asteroidal origin (Morbidelli *et al.* 2002). From these collision intervals, and taking into account (i) that long-period comets collide with the Earth at a velocity that is about three times larger than that of the asteroidal NEOs, (ii) the differences in density and albedo, and (iii) the size distribution of the NEOs, with a back of the envelope calculation we estimate that the dormant long-period comets should not account for more than 1% of the total collisions of given impact energy.

5. CONCLUSIONS

Our recent model of the NEO orbital and magnitude distribution (Bottke *et al.* 2002) indicates that the NEO population is sustained by five intermediate sources, the relative contributions of which are quantitatively determined. In this paper, from the albedo distribution of the bodies in the intermediate NEO sources, we have deduced the albedo distribution of the NEO population.

Our procedure has been complicated by the fact that we do not have direct knowledge of the albedo distribution in the NEO sources. Most radiometric and taxonomic observations concern asteroids that are much bigger than the typical NEO sizes, and there is no reason to believe, a priori, that the albedo distribution of large bodies is representative of smaller objects. Thus, we have been forced to follow a sophisticated extrapolation method to estimate the albedo distribution in the NEO sources for sizes typical of hazardous NEOs. We have tested and constrained our estimates using (i) the color vs heliocentric distance distribution of main belt asteroids given by the SDSS (Ivezić *et al.* 2001) and (ii) published albedo and taxonomic class determinations of NEOs. The results of these comparisons are reasonable enough that we believe our albedo distribution model is an accurate description of reality.

With our albedo distribution model, we predict that the debiased dark/bright (or C/S) ratio of the NEO population is 0.25 ± 0.02 if computed for an absolute-magnitude-limited population and 0.87 ± 0.05 if computed for a size-limited population. Using these values, we estimate that the number of NEOs larger than 1 km in diameter should be 855 ± 110 , roughly 90% of the number of NEOs with absolute magnitude $H < 18$. By assuming values of the bulk density correlated with an object's taxonomic class and computing the collision probabilities between Earth and NEOs for various orbital configurations, we estimate that the Earth should suffer a 1000-MT impact once every

$63,000 \pm 8000$ years. This collision hazard is about four times lower (i.e., less hazardous) than previously estimated (Morrison *et al.* 1994) and is carried on average by objects with $H < 20.6$. We estimate that the known NEOs carry only $18 \pm 2\%$ of this overall collision probability.

Our work also shows the need for new observational campaigns to (i) extend our knowledge of the albedo distribution of smaller main belt asteroids and (ii) improve the taxonomy of the known NEO population. In particular we have pointed out that if we compute the dark/bright ratio separately for NEOs in one-magnitude-wide bins (Fig. 4), the results show large and random oscillations. If the last two bins in the H distribution are indicative of a real trend in the dark/bright asteroid ratio, it may call for a refinement of our NEO model and reveal unexpected properties of the main belt population.

ACKNOWLEDGMENTS

This work has been mainly supported by ESA Contract 14018/2000/F/TB. Research funds for William Bottke were provided by NASA Grants NAG5-9951 and NAG5-10603. R. Jedicke is supported by grants to the Spacewatch Project from NASA (NAG5-7854 and NAG5-8095), AFOSR (F49620-00-1-0126), The David and Lucile Packard Foundation, The Steven and Michele Kirsch Foundation, John and Ilene Nitardy, and other contributors. E. F. Tedesco's portion of the work was supported by Grant AST 0073837 from the National Science Foundation. We are grateful to D. Vokrouhlicky, H. F. Levison, and an anonymous reviewer for carefully reading the manuscript and providing valuable suggestions. The first author also thanks R. Binzel, M. DiMartino, and D. Lazzaro for illuminating discussions.

REFERENCES

- Belton, M., C. Chapman, P. Thomas, M. Davies, R. Greenberg, K. Klaasen, D. Byrnes, L. D'Amario, S. Synnott, W. Merline, J. M. Petit, A. Storrs, and B. Zellner 1995. The bulk density of Asteroid 243 Ida from Dactyl's orbit. *Nature* **374**, 785–788.
- Bottke, W. F., M. C. Nolan, R. Greenberg, and R. A. Kolvoord 1994a. Velocity distributions among colliding asteroids. *Icarus* **107**, 255–268.
- Bottke, W. F., M. C. Nolan, R. Greenberg, and R. A. Kolvoord 1994b. Collisional lifetimes and impact statistics of near-Earth asteroids. In *Hazards due to Comets and Asteroids* (T. Gehrels and M. S. Matthews, Eds.), pp. 337–357. Univ. of Arizona Press, Tucson.
- Bottke, W. F., R. Jedicke, A. Morbidelli, J. M. Petit, and B. Gladman 2000. Understanding the distribution of near-Earth asteroids. *Science* **288**, 2190–2194.
- Bottke, W. F., A. Morbidelli, R. Jedicke, J. M. Petit, H. F. Levison, P. Michel, and T. S. Metcalfe 2002. Debiased orbital and absolute magnitude distribution of the near Earth objects. *Icarus* **156**, 399–433.
- Bowell, E., B. Hapke, D. Domingue, K. Lumme, J. Peltoniemi, and A. W. Harris 1989. Application of photometric models to asteroids. In *Asteroids II* (R. P. Binzel, T. Gehrels, and M. S. Matthews, Eds.), pp. 524–556. Univ. Arizona Press., Tucson.
- Britt, D. T., D. Yeomans, K. Housen, and G. Consolmagno 2002. Asteroid density, porosity, and structure. In *Asteroids III* (W. F. Bottke, A. Cellino, P. Paolicchi, and R. P. Binzel, Eds.), in press. Univ. of Arizona Press, Tucson.
- Bus, S. J. 1999. *Compositional Structure in the Asteroid Belt*. Ph.D. thesis, MIT, Cambridge, MA.
- Bus, S. J., and R. P. Binzel 1998. A feature-based taxonomy derived from 1190 SMASSII CCD spectra. *Am. Astron. Soc. Bull.* **30**, 1025.

- Cellino, A., P. Michel, P. Tanga, and V. Zappalà 1999. The velocity–size relationship for members of asteroid families and implications for the physics of catastrophic collisions. *Icarus* **141**, 79–95.
- D’Abramo, G., A. W. Harris, A. Boattini, S. C. Werner, A. W. Harris, and G. B. Valsecchi 2001. A simple probabilistic model to estimate the population of near Earth asteroids. *Icarus* **153**, 214–217.
- Gradie, J. C., and E. F. Tedesco 1982. Compositional structure of the asteroid belt. *Science* **216**, 1405–1407.
- Greenberg, R. 1982. Orbital interactions—A new geometrical formalism. *Astron. J.* **87**, 184–195.
- Ivezić, Z., S. Tabachnik, R. Rafikov, R. H. Lupton, T. Quinn, M. Hammergren, L. Eyer, J. Chu, J. C. Armstrong, X. Fan, K. Finlator, T. R. Geballe, J. E. Gunn, G. S. Hennessy, G. R. Knapp, S. K. Leggett, J. A. Munn, J. R. Pier, C. M. Rockosi, D. P. Schneider, M. A. Strauss, B. Yanny, J. Brinkmann, I. Csabai, R. B. Hindsley, S. Kent, B. Margon, T. A. McKay, J. A. Smith, P. Waddell, and D. G. York 2001. Solar system objects observed in the Sloan digital sky survey commissioning data. *Astron. J.* **122**, 2749–2784.
- Jedicke, R. 1996. Detection of near Earth asteroids based upon their rates of motion. *Astron. J.* **111**, 970–982.
- Jedicke, R., and T. S. Metcalfe 1998. The orbital and absolute magnitude distributions of main belt asteroids. *Icarus* **131**, 245–260.
- Jedicke, R., A. Morbidelli, T. Spahr, J. M. Petit, and W. F. Bottke 2002. Earth and space-based NEO survey simulations: Prospects for achieving the Spaceguard goal. *Icarus*, submitted (available at http://www.obs-nice.fr/morby/Ref_list.html).
- Levison, H. F., A. Morbidelli, L. Dones, R. Jedicke, P. Wiegert, and W. F. Bottke 2002. The mass suicide of nearly-isotropic comets. *Science*, in press.
- Lupishko, D. F., and M. DiMartino 1998. Physical properties of near-Earth asteroids. *Planet. Space Sci.* **46**, 47–74.
- Luu, J., and D. Jewitt 1989. On the relative numbers of C types and S types among near-Earth asteroids. *Astron. J.* **98**, 1905–1911.
- Marzari, F., P. Farinella, and D. R. Davis 1999. Origin, aging, and death of asteroid families. *Icarus* **142**, 63–77.
- Merline, W. J., L. M. Close, C. Dumas, C. R. Chapman, F. Roddier, F. Menard, D. C. Slater, G. Duvert, C. Shelton, and T. Morgan 1999. Discovery of a moon orbiting the asteroid 45 Eugenia. *Nature* **401**, 565–568.
- Milani, A., and S. Baccili 1998. Dynamics of Earth-crossing asteroids: The protected Toro orbits. *Celest. Mech. Dynam. Astron.* **71**, 35–53.
- Milani, A., S. R. Chesley, and G. B. Valsecchi 1999. Close approaches of Asteroid 1999 AN₁₀: Resonant and non-resonant returns. *Astron. Astrophys.* **346**, L65–68.
- Morbidelli, A., and B. Gladman 1998. Orbital and temporal distribution of meteorites originating in the asteroid belt. *Meteorol. Planet. Sci.* **33**, 999–1016.
- Morbidelli, A., W. F. Bottke, P. Michel, and Ch. Froeschlé 2002. Origin and evolution of near Earth objects. In *Asteroids III* (W. F. Bottke, A. Cellino, P. Paolicchi, and R. P. Binzel, Eds.), in press. Univ. of Arizona press, Tucson.
- Morrison, D. 1992. *The Spaceguard Survey: Report of the NASA International Near-Earth-Object Detection Workshop*. JPL QB651, No. 37, Jet Propulsion Lab., Pasadena, CA.
- Morrison, D., C. R. Chapman, and P. Slovic 1994. The impact hazard. In *Hazards due to Comets and Asteroids* (T. Gehrels and M. S. Matthews, Ed.), pp. 59–91. Univ. of Arizona Press, Tucson.
- NEO Taskforce 2000. *Potentially Hazardous Near Earth Objects*. British National Space Center, London.
- Öpik, E. J. 1951. Collision probabilities with the planets and the distribution of interplanetary matter. *Proc. R. Irish Acad.* **54A**, 165–199.
- Rabinowitz D., E. Helin, K. Lawrence, and S. Pravdo 2000. A reduced estimate of the number of kilometre-sized near-Earth asteroids. *Nature* **403**, 165–166.
- Rivkin, A. S., E. S. Howell, F. Vilas, and L. A. Lebofsky 2002. Hydrated minerals on asteroids: The astronomical record. In *Asteroids III* (W. F. Bottke, A. Cellino, P. Paolicchi, and R. P. Binzel, Eds.), in press. Univ. of Arizona Press, Tucson.
- Shoemaker, E. M. 1983. Asteroid and comet bombardment of the Earth. *Annu. Rev. Earth Planet. Sci.* **11**, 461–494.
- Shoemaker, E. M., R. F. Wolfe, and C. F. Shoemaker 1990. Asteroid and comet flux in the neighborhood of Earth. In *Global Catastrophes in Earth History* (V. L. Sharpton and P. D. Ward, Eds.), Geol. Soc. Am. Spec. Paper 247, pp. 335–342. Geol. Soc. Am., Boulder, Co.
- Stuart, J. S. 2001. Near-Earth asteroid population estimate from the LINEAR survey. *Science* **294**, 1691–1693.
- Tanga, P., A. Cellino, P. Michel, V. Zappalà, P. Paolicchi, and A. Dell’Oro 1999. On the size distribution of asteroid families: The role of geometry. *Icarus* **141**, 65–78.
- Tedesco, E. F. 1994. Asteroid albedos and diameters. In *Asteroids, Comets, Meteorites* (A. Milani, M. DiMartino, and A. Cellino, Eds.), pp. 55–74. Kluwer, London.
- Tedesco, E. F., and J. C. Gradie 2002. Albedos and diameters for 350 asteroids from the IRTF 10 and 20 μm radiometry survey. *Astron. J.*, to be submitted.
- Tedesco, E. F., A. Cellino, and V. Zappalà 2002a. The statistical asteroid model. I: The main belt population for diameters greater than 1 km. *Astron. J.*, to be submitted.
- Tedesco, E. F., P. V. Noah, M. Noah, and S. D. Price 2002b. The Supplemental IRAS Minor Planet Survey (SIMPS). *Astron. J.* **123**, 1056–1085.
- Thomas, P. C., J. Joseph, B. Carcich, B. E. Clark, J. Veverka, J. K. Miller, W. Owen, B. Williams, and M. Robinson 2000. The shape of Eros from NEAR imaging data. *Icarus* **145**, 348–350.
- Yeomans, D. K., J. P. Barriot, D. W. Dunham, R. W. Farquhar, J. D. Giorgini, C. E. Helfrich, A. S. Konopliv, J. V. McAdams, J. K. Miller, W. Owen, D. J. Scheeres, S. P. Synnott, and B. G. Williams 1997. Estimating the mass of Asteroid 253 Mathilde from tracking data during the NEAR flyby. *Science* **278**, 2106–2109.
- Wetherill, G. W. 1967. Collisions in the asteroid belt. *J. Geophys. Res.* **72**, 2429–2444.
- Zappalà, V., P. Bendjoya, A. Cellino, P. Farinella, and C. Froeschlé 1995. Asteroid families: Search of a 12,487-asteroid sample using two different clustering techniques. *Icarus* **116**, 291–314.